ORGANOMETALLICS

Article

pubs.acs.org/Organometallics

Convergent (De)Hydrogenative Pathways via a Rhodium α-Hydroxylalkyl Complex

Simon Sung,[†] Jie Kang Boon,[†] Johnathan J. C. Lee,[†] Nasir A. Rajabi,[‡] Stuart A. Macgregor,[‡] Tobias Krämer,[‡,*] and Rowan D. Young[†,*]

[†]Department of Chemistry, National University of Singapore, 3 Science Drive 3, 117543 Singapore

[‡]Institute of Chemical Sciences, Heriot-Watt University, Edinburgh EH14 4AS, United Kingdom

Supporting Information

ABSTRACT: We report the convergent reaction pathways between [RhH(PPh$_3$)$_4$] and POP ketone (**1**) and alcohol (**2**) ligands that terminate in the formation of an α-hydroxylalkyl rhodium(I) complex (**3**), representing two halves of a formal reduction/oxidation pathway between **1** and **2**. In the case of hydride transfer to **1**, the formation of the α-hydroxylalkyl rhodium(I) complex (**3**) proceeds via a rare hydrido(η^2-carbonyl) complex (**4**). C−H activation in **2** at the proligand's central methine position, rather than O−H activation of the hydroxy motif, followed by loss of dihydrogen also generates the α-hydroxylalkyl rhodium(I) complex (**3**). The validity of the postulated reaction pathways is probed with DFT calculations. The observed reactivity supports α-hydroxylalkyl complexes as competent intermediates in ketone hydrogenation catalyzed by rhodium hydrides and suggest that ligands **1** and **2** may be "noninnocent" coligands in reported hydrogenation catalyst systems in which they are utilized.

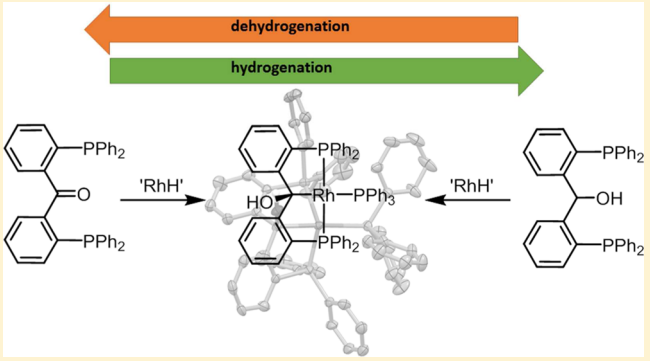

INTRODUCTION

The transfer of hydrogen from metals to ketones and, through reversibility, from alcohols to metals is of fundamental importance to (de)hydrogenation reactions mediated by metal catalysts.[1] Such reactions involve metal hydride intermediates and can proceed via two distinct pathways involving hydride transfer to either the electrophilic carbon or the nucleophilic oxygen of the carbonyl group (Scheme 1).

Scheme 1. Ketone Hydrogenation Proceeding via an Alkoxide Intermediate (Route A) or an α-Hydroxylalkyl Intermediate (Route B)

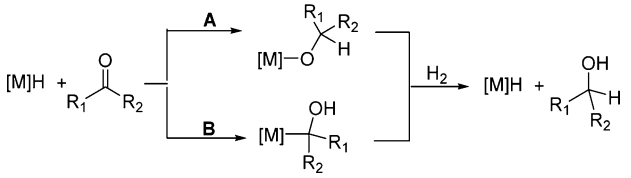

Thus, basic metal monohydrides tend to form metal alkoxide intermediates with ketones (Scheme 1, route **A**); H_2 addition then gives the alcohol product and regenerates the metal hydride.[2,3] In contrast, hydrogenation of aldehydes and ketones with acidic metal hydrides has been observed to proceed via α-hydroxylalkyl intermediates in acidic media (Scheme 1, route **B**).[4]

The mechanism by which a metal hydride is transferred to a bound ketone or aldehyde for cases operating via alkoxide intermediates is well-studied spectroscopically *in situ* and computationally (Scheme 1, **A**).[5] However, the transfer of a metal hydride to generate an α-hydroxylalkyl intermediate has less precedent despite their inference in catalytic hydrogenation[3a,b] and hydroformylation[6] reactions.

Indeed, structurally characterized examples mapping hydride migration to either electrophilic or nucleophilic positions of a bound organocarbonyl are unknown. Intermediates involved in such transitions are of great importance to a wide range of carbonyl reductions but until this study have only been interrogated *in silico* or observed spectroscopically *in situ*.[6]

α-Hydroxylalkyl complexes are typically unstable with respect to β-hydrogen elimination, so examples of isolated complexes are rare.[7] In pioneering work, Gladysz et al. (and later Garralda et al.) demonstrated the formation of α-hydroxylalkyl complexes in constrained environments based on hydride migration to *o*-(diphenylphosphino)benzaldehyde ligands.[7a,b]

If α-hydroxylalkyl complexes lie on the reaction pathway of ketone hydrogenation, then they should also be accessible through the C−H activation of an alcohol. Such selective activation of C−H bonds in the presence of O−H bonds is of great interest regarding simple alcohol functionalization, with

Received: February 28, 2017
Published: April 14, 2017

Downloaded via MAYNOOTH UNIV on November 4, 2019 at 11:38:28 (UTC).
See https://pubs.acs.org/sharingguidelines for options on how to legitimately share published articles.

© 2017 American Chemical Society

DOI: 10.1021/acs.organomet.7b00158
Organometallics 2017, 36, 1609−1617

Scheme 2. Formation of 3 from Addition of 1 or 2 to $[RhH(PPh_3)_4]$[a]

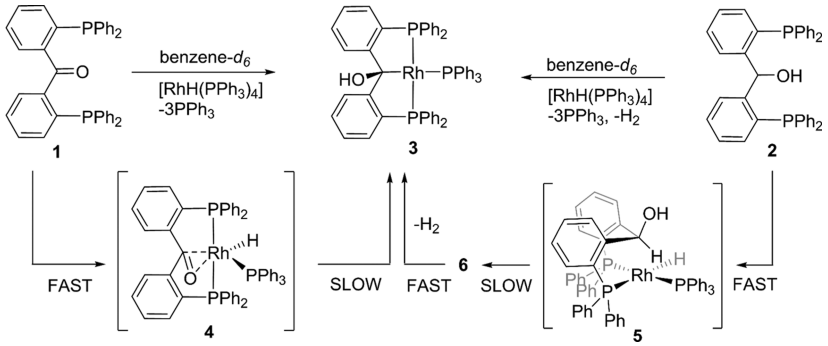

[a]Geometry of compound **6** is discussed below.

the single-step C−H activation and functionalization of alcohol geminal C−H positions remaining a contemporary chemical challenge.[8] However, such selective C−H activation is unknown, so this approach is nontrivial due to the presence of several alternative reaction outcomes.

Herein we describe the controlled hydrogen transfer to and from the ketone and alcohol moieties of the diphosphine POP ligands **1**[9] and **2**[10] mediated by hydridotetrakis(triphenylphosphine)rhodium(I), $[RhH(PPh_3)_4]$. The results demonstrate a convergent pathway to a common α-hydroxylalkyl complex that is accessible from both ketone and alcohol precursors using a common ligand platform. Within this we demonstrate the formation of an α-hydroxylalkyl species direct from a rare isolated metal-hydride/η^2-ketone precursor, as well as the geminal C−H activation of an alcohol. DFT calculations are utilized to probe the mechanistic details of these processes which are shown to map out fully route **B** shown in Scheme 1. The results also highlight the potential noninnocence of these POP ligands, which are commonly used in asymmetric hydrogenation catalysis.[9]

RESULTS AND DISCUSSION

Addition of POP ketone **1** to $[RhH(PPh_3)_4]$ in benzene-d_6 resulted in the loss of 3 equiv of PPh_3 and the formation of the α-hydroxyl complex **3** over 12 h. Monitoring the reaction at shorter time intervals revealed that **1** and $[RhH(PPh_3)_4]$ initially formed hydrido(η^2-carbonyl) **4** (within minutes) that was converted into **3** over a matter of hours at room temperature (Scheme 2). Formation of **4** was evident by the presence of a rhodium-bound carbon (δ_C 137.8, $^1J_{RhC}$ = 9.2 Hz). The chemical shift and rhodium−carbon coupling constant deviate notably from that of the proligand carbonyl (δ_C 197.3) and imply a bonding mode lying between the extreme cases of η^2-carbonyl and metallaepoxide (defined by the Dewar−Chatt−Duncanson model) and exemplified by recently reported analogues [**1**-Ni(PPh_3)][11] and [L_1IrX][12] (L_1 = κ^3-*P*,(η^2-C,O),*P*′-bis(5-(diisopropylphosphino)3,4-benzo[*b*]-thiophenyl)-methanone, X = Cl or OH). A degree of π-retrodonation to the carbonyl is supported by relatively small one-bond rhodium−phosphorus coupling constants ($^1J_{RhP}$ = 130.6, 108.9 Hz) in **4** indicating an electron-poor rhodium center. FTIR spectroscopy could not provide support for carbonyl coordination with failure to identify a specific C=O stretching band. However, a strong Rh−H stretch was observed at 1969 cm^{-1} (cf. calcd value of 1993 cm^{-1}, see Supporting Information).

Crystals of compound **4** were grown upon layering a toluene solution of **4** with hexane at low temperature (253 K). The molecular structure of **4** (Figure 1) supports the coordination

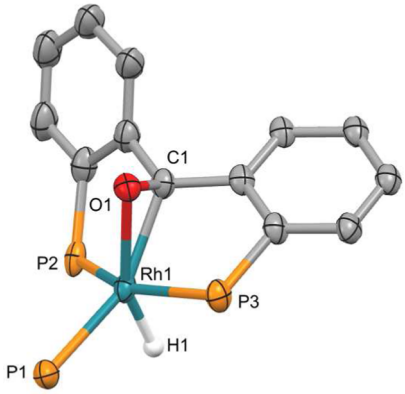

Figure 1. Molecular structure of **4**. Phenyl groups and hydrogens except H1 are omitted for clarity; 50% thermal ellipsoids. H1 was located in a Fourier difference map. Selected distances (Å) and angles (deg): Rh1−C1, 2.118(7); Rh1−O1, 2.187(5); Rh1−P1, 2.382(2); Rh1−P2, 2.318(2); Rh1−P3, 2.262(2); C1−O1, 1.339(8); P2−Rh1−P3, 153.19(8); P1−Rh1−C1, P1, 152.3(2).

of the carbonyl to rhodium, observed spectroscopically in solution. The geometry around rhodium is best described as pseudotrigonal bipyramidal, with numerous examples of analogous pentacoordinate rhodium complexes subtended by η^2-olefin ligands exhibiting such geometry.[13] Significant elongation of the C=O bond (1.339(8) Å) from the free ligand **1** (1.213(3) Å)[9] is observed indicating a significant degree of π-retrodonation. However, the coordination is consistent with a bound carbonyl, falling within the range of previously reported rhodium η^2-carbonyl complexes.[14] Notably, the molecular structure of **4** reveals the hydrido ligand to be *trans* to the oxygen in the coordinated carbonyl, representing a barrier for hydride to carbonyl migration.

In solution, α-hydroxylalkyl complex **3** is generated from **4** upon the transfer of hydrogen from rhodium to oxygen. The ^1H NMR spectrum of compound **3** exhibits a hydroxyl resonance at 3.15 ppm ($^4J_{PH}$ = 3.5 Hz). Selective decoupling of a phosphorus signal at δ_P 37.5 resolves the signal at δ_H 3.15 into a singlet, indicative of long-range $^1H-^{31}P$ coupling. The addition of D_2O to a solution of **3** resulted in the disappearance of this signal, while other NMR signals remained unaffected. The carbon−rhodium bond in **3** is characterized by a doublet

DOI: 10.1021/acs.organomet.7b00158
Organometallics 2017, 36, 1609−1617

of doublet of triplets signal in the ^{13}C NMR spectrum at δ_C 106.1 ($^1J_{RhC}$ = 25.2 Hz), with a typical $^1J_{RhC}$ for a rhodium α-hydroxylalkyl moiety.[7b,h,i]

X-ray diffraction study confirms **3** to be an α-hydroxylalkyl complex (Figure 2). In agreement with solution data, **3** assumes

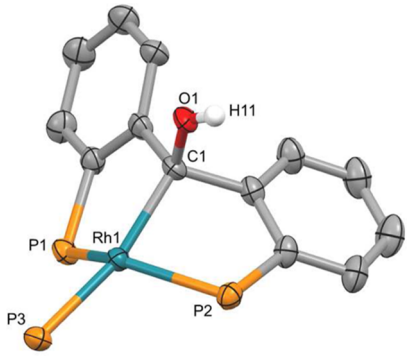

Figure 2. Molecular structure of **3**. Phenyl groups, benzene solvent molecule, and hydrogens except H11 are omitted for clarity; 50% thermal ellipsoids. H11 was located in a Fourier difference map. Selected distances (Å) and angles (deg): Rh1−C1, 2.103(12); C1−O1, 1.458(14); Rh1−P1, 2.231(3); Rh1−P2, 2.254(3); Rh1−P3, 2.315(3); P1−Rh1−P2, 132.45(13); P3−Rh1−C1, 166.4(4); O1−C1−Rh1, 106.4(8).

a distorted square-planar geometry, with P1−Rh1−P2 and C1−Rh1−P3 angles deviating greatly from linear (132.45(13) and 166.4(4)°, respectively). The significantly reduced average Rh−P bond distances in **3** as compared to those in **4** point to a more electron-rich Rh center in the former. The formation of **3** from **4** was monitored with ^1H and ^{31}P NMR spectroscopy across a range of temperatures and in the presence of varying quantities of added PPh_3 (see Supporting Information). Although it was apparent that free PPh_3 accelerated the reaction, the exact reaction order relative to [PPh_3] could not be precisely determined, but it was found to be between 0 and 1. This may be indicative of a nontrivial mechanism. Thus, although accurate activation parameters from these collected data could not be derived, they are discussed in the Supporting Information.

Compound **3** could also be generated by the addition of alcohol proligand **2** to [$RhH(PPh_3)_4$] in benzene-d_6 with concomitant loss of H_2 (Scheme 2). The formation of **3** from **2** and [$RhH(PPh_3)_4$] completes the (de)hydrogenation reaction pathway between **1** and **2** mediated by [$RhH(PPh_3)_4$]. Monitoring the production of **3** from the combination of either **1** or **2** with [$RhH(PPh_3)_4$] reveals that once a maximum concentration of **3** has been achieved very small quantities of **4** are still observed. In the presence of >1 equiv of PPh_3, this equilibrium is established in a matter of days but takes weeks to establish in the absence of PPh_3. The ratio of **3**/**4** after equilibrium is established is ca. 20:1 (see Supporting Information), suggesting a ΔG of −1.8 kcal mol^{-1}.

En route to compound **3** from **2** and [$RhH(PPh_3)_4$], compound **5** is observed. Although **5** is transient at room temperature, at 280 K it can be spectroscopically characterized and is distinguished by the appearance of new signals in the ^1H NMR spectrum at δ_H 9.87 (br s) and 1.39 (d, $^3J_{HH}$ = 3.3 Hz) that correlate to one another in a COSY 2D NMR experiment. A HSQC experiment provided no correlation for the signal at δ_H 1.39 to any ^{13}C atoms but rather correlated the signal at δ_H 9.87 with a signal at δ_C 69.3. These data suggest the identities of the signals at δ_H 9.87 and 1.39 to be the methine CH and OH signals of bound **2** respectively. In the upfield region of the ^1H NMR spectrum of **5**, a broad doublet is observed at δ_H −8.58 ($^2J_{PH}$ = 90 Hz), 0.52 ppm upfield of the hydride signal of [$RhH(PPh_3)_4$] (δ_H −8.06, $^1J_{RhH}$ = 12.7 Hz), suggesting fluxional behavior. The ^{31}P NMR spectrum of **5** further revealed the dynamic behavior of **5**, with two broad doublets present at δ_P 34.3 ($^1J_{RhP}$ = 170 Hz) and 31.0 ($^1J_{RhP}$ = 131 Hz) with a combined integral of three phosphorus nuclei relative to free PPh_3 (integration: 3P).

Analysis by ^{31}P NMR spectroscopy of a solution of **5** and liberated PPh_3 generated from [$RhH(PPh_3)_4$] and **2** in toluene-d_8 at 223 K revealed the presence of at least three separate phosphorus environments on rhodium (integration: 4P) with complex coupling patterns in addition to free PPh_3 (integration: 2P). At this temperature, the ^1H spectrum of **5** revealed that fluxional processes were still occurring on the ^1H NMR time scale. The hydridic signal remained broad. However, it had shifted upfield to −12.22 ppm, and the $^2J_{PH}$ for this signal had increased to 110 Hz. Concurrently, the methine CH signal in bound **2** had shifted upfield from δ_H 9.87 to 9.20. Overall, the NMR data imply that **5** exists in equilibrium with its PPh_3 adduct, **5**·PPh_3, and that the adduct may be preferred at lower temperatures.

A downfield shift for C−H bonds in the vicinity of d^8 metals has been observed in bisphosphino methylene ligands related to **2** (that also undergo C−H activation) and has previously been assigned as an anagostic interaction.[15] Assignment based purely on NMR spectroscopic evidence has recently been reported to be misleading; however, we cautiously assign the C−H−Rh interaction as anagostic with supporting computational analysis (see below).[16]

Further insight into the C−H activation of POP alcohol ligand **2** was obtained from its reaction with [$RhCl(COD)PPh_3$] that led to the formation of the hydridochloride **7** alongside free 1,5-cyclooctadiene (Scheme 3). ^1H NMR data

Scheme 3. Reaction of 2 and [$RhCl(COD)PPh_3$] to Form 7[a]

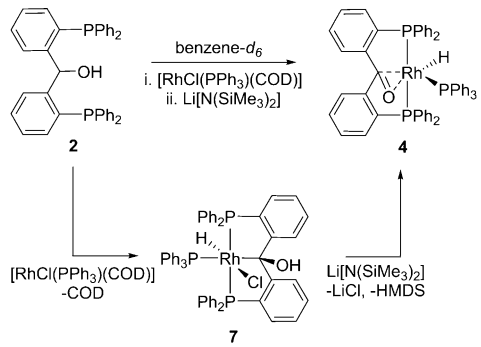

[a]Subsequent treatment of **7** with Li[$N(SiMe_3)_2$] produces **4**.

support compound **7** being an α-hydroxylalkyl complex, with a hydroxyl signal located at δ_H 7.57. This signal appears as a doublet with long-range coupling to phosphorus (d, $^4J_{PH}$ = 7.5 Hz); selective ^{31}P decoupling at δ_P 23.7 collapses this signal to a singlet. The addition of a small quantity of D_2O also resulted in the disappearance of the signal while other NMR data remain unaffected. The ^1H NMR spectrum also reveals the appearance of an upfield hydride shift at δ_H − 16.22 (dtd, $^1J_{RhH}$ = 22.1 Hz (d), $^2J_{PH}$ = 14.3 Hz (t), $^2J_{PH}$ = 9.2 Hz (d)).

DOI: 10.1021/acs.organomet.7b00158
Organometallics 2017, 36, 1609−1617

A molecular structure determination of **7** (Figure 3) reveals its geometry with the PCP ligand adopting a *mer* configuration

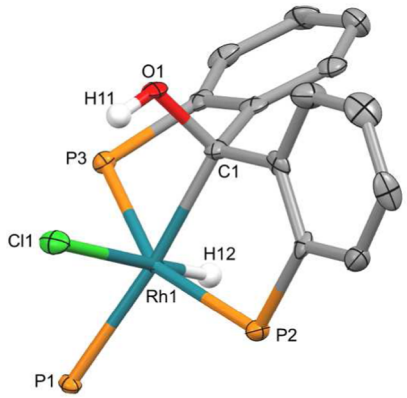

Figure 3. Molecular structure of **7**. Phenyl groups and hydrogens except H11 and H12 are omitted for clarity; 50% thermal ellipsoids. H11 and H12 were located in a Fourier difference map. Selected distances (Å) and angles (deg): Rh1−C1, 2.177(4); Rh1−Cl1, 2.500(1); Rh1−P1, 2.4019(12); Rh1−P2, 2.3189(13); Rh1−P3, 2.2971(12); P2−Rh1−P3, 153.03(4); P1−Rh1−C1, 174.46(12).

after C−H oxidative addition to the rhodium center. It is also observed that the hydroxyl hydrogen (H11), located in a Fourier difference map, is hydrogen-bonded to the proximal chloride ligand (Cl1−$H11_{dist}$ = 2.273 Å). Induced elimination of HCl from **7** by treatment with 1 equiv of $Li[N(SiMe_3)_2]$ results in the formation of compound **4**, which then transforms to **3**. This stands in contrast to the reaction between **2** and $[RhH(PPh_3)_4]$ that generates **3** without any observation of **4**, signifying that H_2 loss occurs via a *cis*-dihydride intermediate rather than through elimination of H_2 from a *trans*-dihydride analogue of **7** (i.e., a *trans*-$Rh^{III}(H)_2(COH)P_2$ fragment).

To investigate the possible identity of *cis*-dihydride intermediate **6**, dihydrogen (4 atm) was introduced into an NMR sample tube containing **3** in toluene-d_8 solution. At room temperature, ^{1}H NMR spectroscopy reveals the formation of a broad signal at δ_H −2.8 (integration: 2H). In addition, the signal for free H_2 (expected at δ_H 4.50) is not observed. The hydroxyl signal originally at δ_H 3.15 is broadened and observed to shift downfield to δ_H 3.65 (integration: 1H). The ^{31}P NMR spectrum of this sample reveals resonances at δ_P 45.6 (dd, 2H, $^1J_{RhP}$ = 125.1 Hz, $^2J_{PP}$ = 20.2 Hz) and 41.7 (dt, 1H, $^1J_{RhP}$ = 93.2 Hz, $^2J_{PP}$ = 20.2 Hz), displaying a similar chemical shift to **3**, but reduced coupling constants. As the temperature is lowered to 233 K, the hydridic signal resolves into a broad doublet at δ_H −6.8 ($^2J_{PH}$ = 140 Hz), indicative of a single *trans* phosphorus-hydride environment. T_1 measurements at various temperatures excluded the identity of **6** as a dihydrogen complex (see Supporting Information). At this temperature, the hydroxyl signal is observed at δ_H 4.25 as a doublet ($^4J_{PH}$ = 4.4 Hz), and free hydrogen is observed as a broad signal at δ_H 4.5 that sharpens at lower temperatures. A $^1H\{^{31}P\}$ NMR spectrum with a decoupling window centered at δ_P 40.0 collapses both the hydridic and hydroxyl signals into singlets.

The ^{31}P NMR spectrum of the sample at 233 K shows a broad doublet at δ_P 45.6 ($^1J_{RhP}$ = 86.5 Hz) and a doublet of triplets at δ_P 41.7 ($^1J_{RhP}$ = 84.5 Hz, $^2J_{PP}$ = 14.9 Hz). HMBC experiment at 233 K (optimized for J_{CH} = 10 Hz) exhibits a correlation between the hydroxyl proton at δ_H 4.25 and a signal at δ_C 95.8. A 1D ^{13}C NMR experiment revealed this signal to be a doublet of doublets ($^2J_{PC}$ = 95.2 Hz, $^1J_{RhC}$ = 28.6 Hz). After warming and degassing of the sample, compound **3** was quantitatively reformed. These data are indicative of the formation of a Rh(III) center at low temperature in dynamic equilibrium with **3** and molecular hydrogen. Given these spectroscopic data, **6** is assigned as a *cis* dihydride featuring a facially coordinated PCP ligand (Scheme 4).[15b,e] Selected NMR spectroscopic data for compound **3**−**7** are shown in Table 1.

Scheme 4. Hydrogenation of 3 Generates *Cis* Dihydride 6

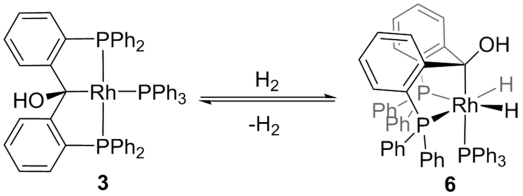

Confirmation that the C−H methine of **2** is activated in reactions with rhodium (as opposed to O−H activation followed by rearrangement) is confirmed by employing isotopologues **2a** and **2b** (Scheme 5).C−H activation is expected on a dehydrogenation pathway that invokes an α-hydroxylalkyl intermediate. When $[RhH(PPh_3)_4]$ is reacted with isotopologue **2a**, **3a** is generated (Scheme 5), which is spectroscopically identical to **3**, except that the RhCO*H* signal at δ_H 3.15 was diminished and a signal at 3.25 ppm was located in the ^{2}H NMR spectrum of **3a**, signifying the deuteration of the hydroxyl position. Conversely, when **2b** is reacted with $[RhH(PPh_3)_4]$, compound **3** is produced with loss of HD. Addition of **2b** to $[RhCl(COD)PPh_3]$ resulted in the production of **7b**, identical to **7** (by NMR spectroscopy) with the exception of substitution of the hydride ligand with deuterium, as evident by the absence of a hydridic signal in the ^{1}H NMR spectrum.

To elucidate the mechanistic details of the convergent pathways that convert both the ketone (**4**) and alcohol (**5**) precursors into the α-hydroxylalkyl product **3**, a computational analysis of the associated free energy surfaces was carried out using DFT calculations at the B97-D3/BS2//BP86/BS1 level of theory corrected for benzene solvent (see Supporting Information for computational details). The most accessible computed pathways at 298 K for both processes are detailed in Figure 4. The optimized structure of **4** agrees well with the crystallographic data. In particular the C═O (calcd: 1.35 Å, exp.: 1.339(8) Å), Rh−C (calcd: 2.16 Å, exp.: 2.118(7) Å), and Rh−O (calcd: 2.22 Å, exp.: 2.187(5) Å) distances are well-reproduced, along with the *trans*-P−Rh−P angle of the POP ligand (calcd: 154.0°, exp.: 153.19(8)°).

Analysis of the natural bond orbitals (NBOs) in **4** shows that C═O coordination to the metal center is governed by $\pi_{CO} \rightarrow$ Rh donation, reinforced by substantial $\pi^*_{CO} \leftarrow$ Rh back-donation (see Figure S65). The elongation of the C═O bond arises due to notable population of the π^*_{CO} orbital (0.79 e^-) and depopulation of the π_{CO} orbital (1.82 e^-). The partial reduction of the double-bond character of the C═O bond is also reflected in the Wiberg bond index (1.18), lying in between those for the C═O double bond in **1** (1.68) and the C−O(H) single bond in **2** (0.91). In contrast, the indices for the Rh···C (0.39) and Rh···O (0.24) interactions are smaller compared to those found for the Rh−C (0.47) and Rh−H (0.56) bonds in **3** and **4**, respectively, which serve as a reference

DOI: 10.1021/acs.organomet.7b00158
Organometallics 2017, 36, 1609−1617

Table 1. Selected NMR Spectroscopic Data for Compounds 3-7

compound	δ_C (Rh−C)	$^2J_{PC}$ (Hz)	$^1J_{RhC}$ (Hz)	J_{RhP} (Hz)	J_{PP} (Hz)
3	106.1	4.8 (t), 73.5 (d)	25.2	189, 120	28.3
4	137.8	23.7 (d)[a]	9.2	131, 109	10.1
5	N/A	N/A	N/A	170, 131[b]	*a*
6	95.8[c]	95.2 (d)[a,c]	28.6[c]	87, 85[c]	14.9[c]
7	99.4	94.1 (d)[a]	20.8	120, 79	24.0

[a]Coupling to *cis* phosphorus nuclei was not observed. [b]280 K. [c]233 K.

Scheme 5. Isotopomers 2a, 2b React with $[RhH(PPh_3)_4]$ to Generate Isotopologues 3a and 7b, Respectively

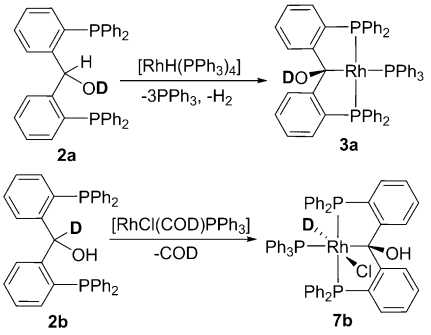

point. Thus, in accordance with the experimental findings the {RhCO} unit is best described as a Rh-bound carbonyl.

The optimized structure of **3** reproduces the distorted square-planar geometry around Rh seen experimentally: *trans*-P−Rh−P (calcd: 132.9°, exp.: 132.45(13); *trans*-C−Rh−P (calcd: 164.1°, exp.: 166.4(4)). The Rh−C distance is reduced from 2.16 Å in **4** to 2.13 Å in **3**, and this is paralleled by an increase in the calculated Rh−C isotropic spin−spin coupling constant (**4**: $^1J_{RhC}$ = −9.1 Hz; **3**: $^1J_{RhC}$ = −17.4 Hz).

The computed mechanism for the formation of **3** from **4** starts with an initial isomerization of **4**, with a calculated barrier of 17.7 kcal mol^{-1} proceeding via **TS(4−Int1)**. The POP ligand undergoes isomerization from a *mer*-κ^3-P,(CO),P to a *fac*-κ^3-P,(CO),P binding mode (∠P−Rh−P 109.1°). Concomitantly, the hydride moves from its equatorial coordination site *trans* to oxygen into the opening axial position. The distortion of the ligand in **TS(4−Int1)** also causes the C═O unit to move away from Rh (Rh−O: 2.52 Å; Rh−C: 2.38 Å), thereby decreasing *π*-backbonding from the metal center and restoring more double-

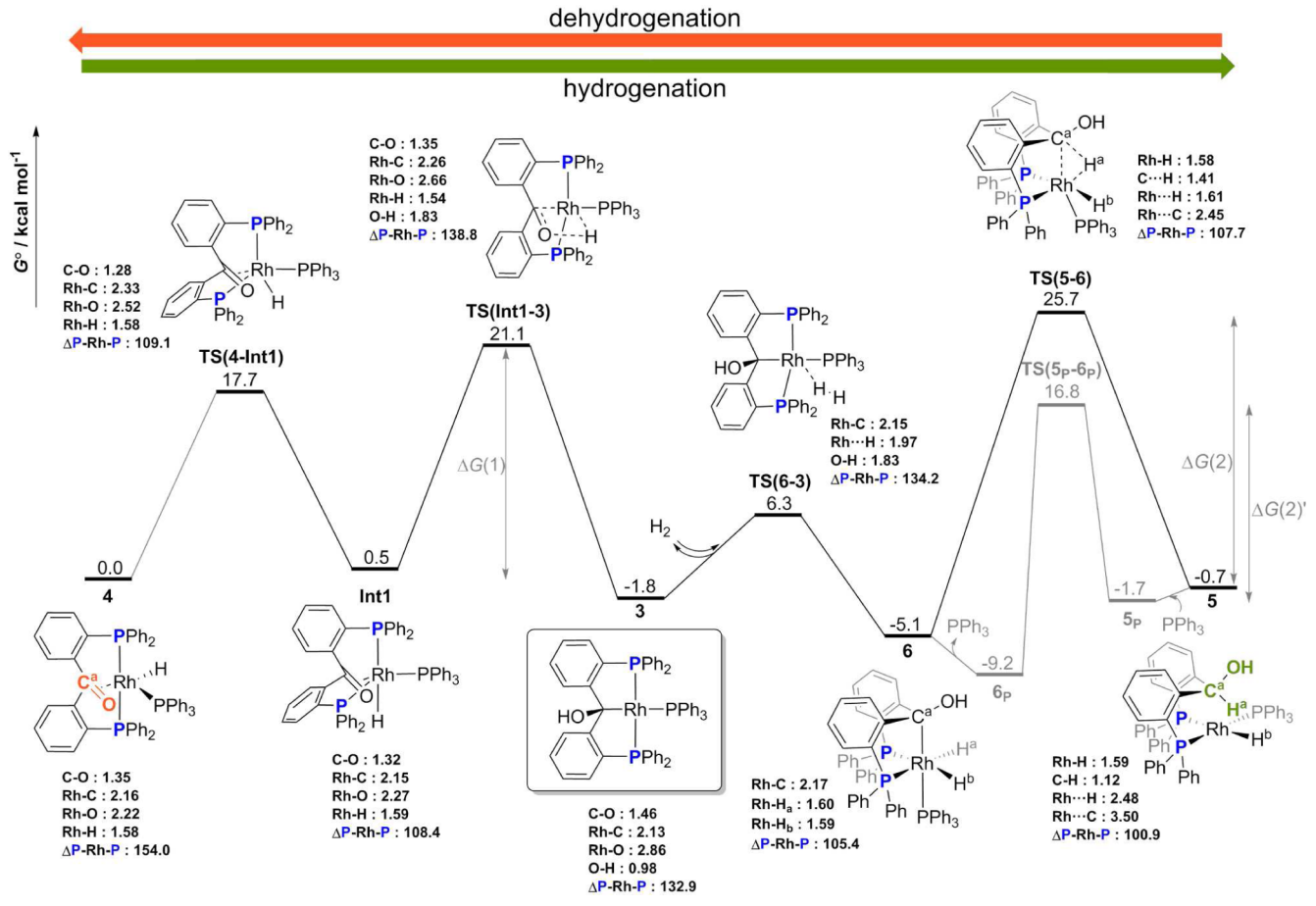

Figure 4. Computed profile (B97-D3/BS2//BP86/BS1) for the transformation of **4** into **3** (left) and **5** into **3** (right). The gray profile is associated with adduct $\mathbf{5_P}$, featuring H-bonded PPh_3. Relative Gibbs free energies (298 K, kcal mol^{-1}), corrected for benzene solvent, are given along with key bond metric data (Å, deg). Double-arrows indicate energy spans $\Delta G(1)$, $\Delta G(2)$, and $\Delta G(2)'$.

DOI: 10.1021/acs.organomet.7b00158
Organometallics 2017, 36, 1609−1617

bond character (C═O: 1.28 Å). The *cis* arrangement of the {Rh(C═O)(H)} moiety in **Int1** ($G°$ = +0.5 kcal mol^{-1}) allows for insertion of the ketone into the Rh−H bond through **TS(Int1−3)** at 21.1 kcal mol^{-1} to form the α-hydroxylalkyl in **3**. By inspection, **TS(Int1−3)** also defines the overall energetic span[17] ($\Delta G(1)$ = +21.1 kcal mol^{-1}) for the transformation of **4** into **3**, with the computed barrier being consistent with the slow process seen experimentally. The hydrogen transfer in **TS(Int1−3)** is accompanied by an isomerization of the ligand to its distorted *mer*-κ^3-P,C,P form (∠P−Rh−P 138.8°). Complex **3** is energetically stabilized by a mere 1.8 kcal mol^{-1} relative to **4**. The marginal exergonicity of this process is in line with the establishment of an equilibrium between these two species, as confirmed by experiment.

The lowest-energy pathway for the formation of **3** from **5** is shown on the right side of Figure 4. Precursor complex **5** features an approximately square-planar geometry around the Rh^{I} center, with the POP ligand adopting a *cis*-κ^2-P,P arrangement (∠P−Rh−P 100.9°) and computed Rh···H^a and Rh···C^a distances of 2.48 and 3.50 Å, respectively, to the central C−H bond of the ligand. Computed AIM and NBO parameters suggest that the Rh···H^a−C^a interaction is of closed-shell electrostatic nature, in line with a weak anagostic interaction.[16,18] Oxidative addition of the C^a−H^a bond across the P$_{POP}$−Rh−PPh$_3$ vector occurs with a barrier of 26.4 kcal mol^{-1} to yield intermediate **6** (−5.1 kcal mol^{-1}). Activation of the C−H bond in **TS(5−6)** is accompanied by movement of the PPh$_3$ ligand into the axial position. We have also considered other possibilities for this reaction step, none of which presented a feasible alternative. Oxidative addition across the P$_{PPh3}$−Rh−H vector in the alternative *trans*-isomer **5′** shifts the energy profile upward by ∼10 kcal mol^{-1} (see Supporting Information). A search for a concerted C−H activation step via σ-bond metathesis proved unsuccessful. Experimentally there is an excess of PPh$_3$ present in solution, so we also scrutinized the possible effect of C(H)OH···PPh$_3$ H-bonding on the C−H activation. Under these circumstances, the barrier is notably lowered ($\Delta G°^{‡}$ = 18.5 kcal mol^{-1}, relative to **5$_P$**, gray profile in Figure 4). The optimized structure of the corresponding transition state **TS(5$_P$-6$_P$)** is shown in Figure 5. The optimized bond parameters in **TS(5$_P$−6$_P$)** closely resemble those in **TS(5−6)**, with Rh···C^a, Rh···H^a, and C^a−H^a distances of 2.45, 1.61, and 1.43 Å, respectively. The (O)H···PPh$_3$ distance is 2.45 Å, similar to the H-bond in complex **5$_P$**. Complex **6** exhibits an octahedral coordination geometry around the Rh^{III} center, featuring a *fac*-κ^3-P,C,P tridentate ligand with the Rh−C bond *trans* to PPh$_3$. Facile reductive elimination of the *cis*-hydrides in **6** proceeds with a barrier of 11.4 kcal mol^{-1} readily generating the final product **3** upon loss of H$_2$. The overall reaction rate is determined by the initial oxidative addition step at 18.5 kcal mol^{-1}, and this reduced barrier is consistent with the observation that **5** is transient at room temperature. Note that although the formation of **3** is computed to be slightly endergonic relative to **6** ($\Delta G°$ = +3.3 kcal mol^{-1}) experimentally species **3** and **6** are in equilibrium which can be driven to **3** by removal of H$_2$ upon degassing the solution.

Experimentally the NMR characterization of **5** points to it being fluxional in solution and, moreover, that temperature-dependent coordination of PPh$_3$ to the Rh center also occurs. Computationally, the trigonal-pyramid and *trans*-κ^2-P,P isomers of **5** lie ∼10 kcal mol^{-1} above the *cis*-isomer, so these may be kinetically accessible in potential H/PPh$_3$ exchange pathways.[19] Formation of a trigonal-bipyramidal 18-electron complex, **5**·PPh$_3$, via axial addition of PPh$_3$ to **5** was computed to be energetically strongly favored ($\Delta G°$ = −7.6 kcal mol^{-1}), even when the basis set superposition error (BSSE) was taken into account. This value runs counter to experimental evidence suggesting a dynamical equilibrium in which PPh$_3$ reversibly binds to **5** (i.e., a thermoneutral process with $\Delta G°$ ≈ 0 kcal mol^{-1}). Although dispersion-corrected DFT can predict phosphine−metal binding energies with good accuracy,[20] in the present example the metal−ligand bond strength appears to be strongly overestimated by the calculations. Of a range of functionals that were tested, B3LYP-D3 performs well for the phosphine binding energy (see Table 2).[20e] However, with this approach the overall barriers linking **4** to **3** and **5** to **3** are in excess of 25 kcal mol^{-1}, rather too high for these room temperature processes. It seems that no single functional can provide balanced energetics for the various ligand binding and bond activation steps in this system. Nonetheless, our conclusions regarding the mechanism for the convergent formation of **3** from **4** and **5**, respectively, obtained with the B97-D3/BS2//BP86/BS1 protocol are qualitatively in good agreement with the experimental observations.

It is plausible that dissociation of PPh$_3$ from **5**·PPh$_3$ must occur prior to C−H bond activation to give **6**. Indeed, a stepwise relaxed scan of the Rh···C^a distance in **5**·PPh$_3$ induces dissociation of one PPh$_3$ ligand, restoring the square-planar geometry of **5** before accessing **TS(5−6)**. The computed intrinsic reaction coordinate clearly confirms that **TS(5−6)** connects **6** to **5** providing support for **5** as an intermediate along the reaction profile.

Table 2. Summary of the Functional Dependence of Phosphine Binding Energies According to 5 + PPh$_3$ ⇆ 5·PPh$_3$ ($\Delta G_{bind+BSSE}$, in kcal mol^{-1}) as Well as Key Energy Spans for the Overall Reaction Profile in Figure 4[a]

functional	$\Delta G_{bind+BSSE}$	$\Delta G(1)$	$\Delta G(2)$	$\Delta G(2)'$
BP86-D3	−13.6	22.2	22.6	14.6
B97-D3	−7.6	21.1	26.4	18.5
B3LYP-D3	+0.1	25.6	29.9	21.5
M06	+8.6	24.9	33.7	24.4

[a]See Figure 4for the definition of ΔG(1), ΔG(2) ΔG(2)′).

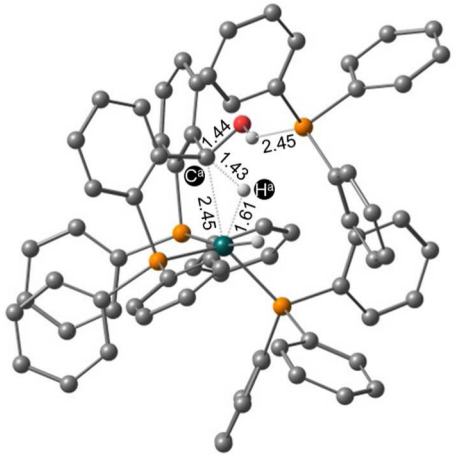

Figure 5. Optimized geometry of **TS(5$_P$−6$_P$)**. Bond distances are in Å.

DOI: 10.1021/acs.organomet.7b00158
Organometallics 2017, 36, 1609−1617

CONCLUSIONS

$[RhH(PPh_3)_4]$ reacts with both the POP ketone (**1**) and POP alcohol (**2**) proligands to produce α-hydroxylalkyl (**3**) through convergent pathways. A number of key intermediates for both branches of this reactivity were either isolated and fully characterized or characterized *in situ* by NMR spectroscopy. In particular, reaction with **1** gives intermediate **4**, a rare example of a trapped η^2-ketone hydrido complex that subsequently undergoes insertion. With **2** the reaction proceeds via C−H activation geminal to the hydroxyl group. Independent synthesis of hydrido chloride complex **7** provided evidence of the feasibility of this novel C−H activation.

The underlying mechanisms were further validated by DFT calculations. These show that the formation of **3** from **4** involves initial *mer-fac*-isomerization of the ligand followed by rate-limiting insertion. For the generation of **3** from POP alcohol precursor **5**, the initial C−H oxidative addition is rate-limiting, and this process is facilitated by the presence of PPh_3 which H-bonds to the C(H)OH moiety of the ligand.

The observed reactivity supports α-hydroxylalkyl complexes as competent intermediates in ketone hydrogenation catalyzed by rhodium hydrides and suggests that **1** and **2** may be "noninnocent" ligands in reported hydrogenation catalyst systems. This work demonstrates a new strategy via ketone insertion to access $PC_{sp3}P$ pincer complexes for metals that disfavor C−H activation. Additionally, the demonstration of C−H activation of a geminal hydroxyl position provides insight into the selective C−H activation in the presence of an alcohol functionality. Ongoing research is being undertaken to determine the reactivity of compound **3** and its analogues, particularly in regards to developing new synthetic routes to $PC_{sp3}P$ and $PC_{sp2}P$ pincer complexes and their potential in catalysis.

EXPERIMENTAL SECTION

General Information. All manipulations were carried out under nitrogen using a glovebox and/or Schlenk techniques. All reactions were performed in glassware that was oven-dried for at least 12 h. Benzene was distilled over sodium and benzophenone under a nitrogen atmosphere and stored over 4 Å molecular sieves prior to use. Diethyl ether and *n*-hexane were dried over activated alumina using an LC Technology Solution Inc. SP-1 Solvent Purification System and deoxygenated prior to use. C_6D_6 used was stirred over CaH_2 at room temperature under a nitrogen atmosphere overnight prior to distillation under reduced pressure and storage over 4 Å molecular sieves. Toluene-d_8 was deoxygenated and stored over 4 Å molecular sieves prior to use. $[RhH(PPh_3)_4]$ and ligands **1** and **2** were prepared according to reported methods.[21]

NMR spectroscopy data were obtained using Bruker AV-300, AV-400, and AV-500 spectrometers. HRMS (ESI-TOF) spectra were obtained using an Agilent Technologies 6230 TOF LC/MS. IR spectroscopy data were obtained using Bruker ALPHA FTIR spectrometers.

Synthesis of Complex 3. **1** (10 mg, 0.018 mmol) and $[RhH(PPh_3)_4]$ (21 mg, 0.018 mmol) were added to a NMR tube under N_2 atmosphere. The components were dissolved in C_6D_6 (0.6 mL) to form an orange solution immediately, which turned green overnight. NMR analyses showed the reaction to be virtually quantitative in the formation of complex **3**. ^{1}H NMR (300 MHz, C_6D_6) = δ_H 3.15 (d, $^4J_{PH}$ = 3.5 Hz, 1H, O*H*), 6.68−7.09 (m, 27H, Ar-*H*), 7.23−7.47 (m, 15H, Ar-*H*), 7.59 (d, $^3J_{HH}$ = 7.8 Hz, 2H, Ar-*H*). $^{13}C\{^1H\}$ NMR (126 MHz, C_6D_6) = δ_C 162.7 (t, J_{PC} = 18.5 Hz), 145.0 (dd, J_{PC} = 19 Hz, 8.5 Hz), 144.6 (d, J_{PC} = 25.3 Hz), 140.0 (d, J_{PC} = 25.2 Hz), 138.9 (d, J_{PC} = 44.2 Hz), 138.7 (d, J_{PC} = 25.7 Hz), 137.3 (t, J_{PC} = 16.0 Hz), 135.1 (s), 134.3 (t, J_{PC} = 11.0 Hz), 133.8 (q, J_{PC} = 6.9 Hz), 131.0 (s), 128.5 (t, J_{CP} = 5.6 Hz), 127.6 (d, J_{CP} = 8.9 Hz), 126.5 (s) 106.1 (ddt, $^2J_{PC}$ = 73.5 (d), 4.8 (t) Hz, $^1J_{RhC}$ = 25.2 Hz). $^{31}P\{^1H\}$ NMR (162 MHz, C_6D_6) = δ_P 37.5 (dt, $^1J_{RhP}$ = 120.4 (d), $^2J_{PP}$ = 28.3 (t) Hz, 1P), 43.3 (dd, $^1J_{RhP}$ = 189.2 (d), $^2J_{PP}$ = 28.3 (d) Hz, 2P). HRMS (ESI-TOF) *m*/*z*: $[M - H]^+$ Calcd for $C_{55}H_{43}OP_3Rh$ 915.1582; Found 915.1546; $[M - OH]^+$ Calcd for $C_{55}H_{43}P_3Rh$ 899.1633; Found 899.1595.

Synthesis of Complex 4. *Method A.* Benzene (5 mL) was added to a mixture of **1** (55.1 mg, 0.100 mmol) and $[RhH(PPh_3)_4]$ (115.3 mg, 0.100 mmol), and the resultant orange solution stirred at room temperature for 30 min, after which the solution was filtered. The filtrate was evaporated to give an orange residue and *n*-hexane (15 mL) was added. After trituration of the mixture for 5 min, the solid was filtered and washed with diethyl ether (2 × 2 mL) and then *n*-hexane (5 × 10 mL). After drying *in vacuo*, the product was isolated as an orange solid (64 mg, 70%).

Method B. $Li[N(SiMe_3)_2]$ (11.7 mg, 0.07 mmol) was added to solution of **7** (66.7 mg, 0.07 mmol) in C_6H_6 (5 mL) at room temperature and stirred for 15 min. The solution was rapidly evaporated under vacuum, and then diethyl ether (5 mL) was added. After trituration of the mixture for 5 min, the solid was filtered and washed with diethyl ether (2 mL) and then *n*-hexane (2 × 10 mL). After drying in vacuo, product **4** was isolated as an orange solid (35 mg, 55%). ^{1}H NMR (500 MHz, C_6D_6) = δ_H −13.27 (ddt, $^1J_{RhH}$ = 21.2 (d), $^2J_{PH}$ = 10.3 (d), $^2J_{PH}$ = 4.2 (d) Hz, 1H, Rh-*H*), 6.64−7.04 (m, 31H, Ar-*H*), 7.48−7.55 (m, 6H, Ar-*H*), 7.59−7.67 (m, 4H, Ar-*H*), 8.05 (d, $^3J_{H-H}$ = 8.0 Hz, 2H, Ar-*H*). $^{13}C\{^1H\}$ NMR (126 MHz, C_6D_6) = δ_C 156.8 (t, J_{PC} = 13.0 Hz), 137.8 (dd, $^1J_{RhC}$ = 23.7 (d), $^2J_{PC}$ = 9.2 (d) Hz), 137.1 (m), 134.7 (d, J_{PC} = 13.5 Hz), 133.8 (s), 133.4 (dt, J_{PC} = 20.0 (d), 6.9 (t) Hz), 129.1 (s), 128.9 (s), 128.4 (s), 128.2 (d, J_{PC} = 28.7 Hz), 127.4 (d, J_{PC} = 8.3 Hz), 127.3 (t, J_{PC} = 4.1 Hz), 126.0 (m), 125.4 (s). $^{31}P\{^1H\}$ NMR (162 MHz, C_6D_6) = δ_P 31.0 (dt, $^1J_{RhP}$ = 108.9 (d), $^2J_{PP}$ = 10.1 (t) Hz, 1P), 40.4 (dd, $^1J_{RhP}$ = 130.6 (d), $^2J_{PP}$ = 10.1 (d) Hz, 2P). IR (nujol mull): 1969 [ν(Rh−H)] cm^{-1}; HRMS (ESI-TOF) *m*/*z*: $[M + H]^+$ Calcd for $C_{55}H_{45}OP_3Rh$ 917.1738; Found 917.1736.

Synthesis of Complex 7. Benzene (2 mL) was added to a mixture of **2** (27.6 mg, 0.05 mmol) and $[RhCl(PPh_3)(COD)]$ (25.4 mg, 0.05 mmol), and the resultant solution was stirred at room temperature for 1 h. The solution was concentrated under vacuum to give a residue, and then *n*-hexane (5 mL) was added to produce a precipitate. The solid was filtered and washed with *n*-hexane (3 × 5 mL). After drying *in vacuo*, the product was isolated as yellow-brown solid (31 mg, 65%). ^{1}H NMR (500 MHz, C_6D_6) = δ_H −16.22 (1 H, dtd, $^1J_{RhH}$ = 22.1 Hz (d), $^2J_{PH}$ = 14.3 Hz (t), $^2J_{PH}$ = 9.2 Hz (d), Rh-*H*), 7.57 (1 H, d, J_{PH} = 7.5 Hz, O*H*), 8.2−6.6 (43 H, m, Ar-*H*). $^{13}C\{^1H\}$ NMR (126 MHz, C_6D_6) = δ_C 163.9 (t, J_{PC} = 15 Hz), 141.9 (t, J_{PC} = 25 Hz), 136.4 (t, J_{PC} = 24 Hz), 135.1 (s (br)), 134.4 (t, J_{PC} = 5.6 Hz), 133.6 (t, J_{PC} = 5.6 Hz), 133.0 (s), 130.0 (s (br)), 129.2 (s), 129.1 (s), 128.9 (s), 128.3 (s), 127.3 (d, J_{PC} = 8.4 Hz), 124.4 (s (br)), 99.4 (dd, J_{PC} = 94.1 Hz, J_{RhC} = 20.8 Hz). $^{31}P\{^1H\}$ NMR (202 MHz, C_6D_6) = δ 39.7 (dd, J_{RhP} = 120.0 Hz, J_{PP} = 24.0 Hz, 2 P), 23.7 (dt, J_{RhP} = 79.0 Hz, J_{PP} = 24.0 Hz, 1 P). IR (nujol mull): 2079 [ν(Rh−H)], 3303 [ν(O−H)] cm^{-1}. HRMS (ESI-TOF) *m*/*z*: [M − Hydride]$^+$ Calcd for $C_{55}H_{44}ClOP_3Rh$ 951.1349; Found 951.1335; $[M - Cl]^+$ Calcd for $C_{55}H_{45}OP_3Rh$ 917.1738; Found 917.1703.

***In Situ* Characterization of Complex 5.** **2** (10 mg, 0.018 mmol) and $[RhH(PPh_3)_4]$ (21 mg, 0.018 mmol) were added into a NMR tube under N_2 atmosphere. The components were dissolved in C_6D_6 (0.6 mL) and then analyzed soon after. The NMR spectroscopic data were obtained at 280 K to reduce the rate of conversion from intermediate **5** to complex **3**. ^{1}H NMR (500 MHz, C_6D_6) = δ_H −8.58 (1 H, d (br), $^2J_{PH}$ = 90 Hz, Rh-*H*), 1.39 (1 H, d, $^3J_{HH}$ = 3.3 Hz, O*H*), 8.0−6.2 (43 H, m, Ar-*H*), 9.87 (1 H, s (br), C(OH)-*H*). ^{1}H−^{1}H COSY NMR shows strong correlation between signals at δ_H 9.87 and 1.39. The doublet at δ_H 1.39 is not resolved upon broadband ^{31}P decoupling. Selected ^{13}C NMR data (from HMBC/HSQC) = δ_C 69.3 (C), 147.4 (C). $^{31}P\{^1H\}$ NMR (202 MHz, C_6D_6) = δ_P 31.0 (d (br), $^1J_{RhP}$ = 131 Hz), 34.3 (d (br), $^1J_{RhP}$ = 170 Hz).

DOI: 10.1021/acs.organomet.7b00158
Organometallics 2017, 36, 1609−1617

***In Situ* Characterization of Complex 6.** To a sample of **3** prepared from **1** and $[RhH(PPh_3)_4]$ in toluene-d_8 (0.6 mL) as described above was applied a pressure of hydrogen gas (4 atm). The sample was then analyzed using VT-NMR spectroscopic experiments. Selected NMR spectroscopic data for **6** at 233 K: ^{1}H NMR (500 MHz, C_6D_6) = δ_H −6.8 (2 H, d (br), $^2J_{PH}$ = 140 Hz, Rh-*H*), 4.25 (1 H, d, $^4J_{PH}$ = 4.4 Hz, O*H*). ^{13}C NMR data (from HMBC) = δ_C 95.8 (1 C, dd, $^2J_{PC}$ = 95.2 Hz, $^1J_{RhC}$ = 28.6 Hz, Rh-C−OH). ^{31}P{^{1}H} NMR (202 MHz, C_6D_6) = δ_P 45.6 (d (br), $^1J_{RhP}$ = 86.5 Hz), 41.7 (dt, $^1J_{RhP}$ = 84.5 Hz, $^2J_{PP}$ = 14.9 Hz).

Preparation of Deuterium-Labeled Ligand 2a. A 1:1 mixture of D_2O/THF was added to **2** followed by evaporation to dryness. Approximately 81% deuteration of the hydroxyl position at 2.25 ppm was determined by ^{1}H NMR spectroscopy. ^{1}H NMR (400 MHz, C_6D_6) = δ_H 6.89 (td, *J* = 7.5, 1.4 Hz, 2H, Ar-*H*), 6.94−7.06 (m, 14H, Ar-*H*), 7.19−7.24 (m, 2H, Ar-*H*), 7.27−7.37 (m, 8H, Ar-*H*), 7.50−7.56 (m, 2H, Ar-*H*), 7.76 (t, *J* = 6.2 Hz, 1H, C(OH)-*H*). ^{31}P{^{1}H} NMR (162 MHz, C_6D_6) = δ_P −17.3 (s, 2 P).

Preparation of Deuterium-Labeled Ligand 2b. *Part A.* (2-Bromophenyl)diphenylphosphene (2.00 g, 5.9 mmol) was dissolved in diethyl ether (25 mL). The solution is then treated dropwise with *n*-BuLi in hexane (6 mL, 1.6 M, 9.6 mmol) at −78 °C and stirred for 30 min. Dimethylformamide-d_7 (3 mL, 38.6 mmol) was added thereafter at −78 °C. The mixture was then allowed to come to room temperature and was stirred overnight. Dilute aqueous HCl solution (20 mL) was added, and then the aldehyde product was extracted using DCM (3 × 30 mL). The combined extractions were dried with Na_2SO_4 and then evaporated. The crude product was then recrystallized using methanol to give *deutero* 2-(diphenylphosphino)-benzaldehyde (0.901 g, 52%).

Part B. (2-Bromophenyl)diphenylphosphine (0.423 g, 1.24 mmol) was dissolved in diethyl ether (10 mL) and treated with *n*-BuLi (2.9 mL, 1.6 M, 1.78 mmol) at 0 °C. The reaction mixture was stirred for 30 min; thereafter, *deutero* 2-(diphenylphosphino)benzaldehyde (0.519 g, 1.78 mmol) was added. The reaction mixture was then stirred for an additional hour. The mixture is then allowed to come to room temperature, and degassed dilute aqueous HCl solution was added. Then, the product was extracted with diethyl ether (3 × 20 mL). The solvent was removed under vacuum and the crude product was recrystallized using methanol to give ligand **2b** as a white solid (0.136 g, 20%). ^{1}H NMR (400 MHz, C_6D_6) = δ_H 2.25 (t, *J* = 1.4 Hz, 1H, O*H*), 6.89 (td, *J* = 7.5, 1.4 Hz, 2H, Ar-*H*), 6.94−7.09 (m, 14H, Ar-*H*), 7.18−7.24 (m, 2H, Ar-*H*), 7.26−7.37 (m, 8H, Ar-*H*), 7.49−7.56 (m, 2H, Ar-*H*). ^{31}P{^{1}H} NMR (162 MHz, C_6D_6) = δ_P −17.3 (s, 2 P).

■ ASSOCIATED CONTENT

Supporting Information

The Supporting Information is available free of charge on the ACS Publications website at DOI: 10.1021/acs.organomet.7b00158.

Experimental methods, formation and isolation details, NMR monitoring details and spectra, HRMS spectra, X-ray crystallography data, and DFT calculations (PDF)

Crystallographic information files for **3**, **4**, and **7** (CIF)

Cartesian coordinates for **4** (XYZ)

■ AUTHOR INFORMATION

Corresponding Authors

*E-mail: t.kraemer@hw.ac.uk.

*E-mail: rowan.young@nus.edu.sg.

ORCID

Simon Sung: 0000-0002-7864-7694

Stuart A. Macgregor: 0000-0003-3454-6776

Tobias Krämer: 0000-0001-5842-9553

Rowan D. Young: 0000-0001-7437-8944

Notes

The authors declare no competing financial interest.

■ ACKNOWLEDGMENTS

We thank the National University of Singapore and the Singapore Ministry of Education for financial support (WBS R-143-000-586-112 and R-143-000-666-114) and Heriot-Watt University for the award of a James Watt Scholarship.

■ REFERENCES

(1) (a) Birch, A. J.; Williamson, D. H. In *Organic Reactions*; John Wiley & Sons, Inc.: Hoboken, NJ, 2011. (b) de Vries, J. G.; Elsevier, C. J. *The Handbook of Homogeneous Hydrogenation*; Wiley-VCH: Weinheim, 2007.

(2) (a) Schrock, R. R.; Osborn, J. A. *J. Chem. Soc. D* **1970**, 567. (b) Malacea, R.; Poli, R.; Manoury, E. *Coord. Chem. Rev.* **2010**, *254*, 729. (c) Samec, J. S. M.; Bäckvall, J.-E.; Andersson, P. G.; Brandt, P. *Chem. Soc. Rev.* **2006**, *35*, 237. (d) Clapham, S. E.; Hadzovic, A.; Morris, R. H. *Coord. Chem. Rev.* **2004**, *248*, 2201. (e) Gregorio, G.; Pregaglia, G.; Ugo, R. *Inorg. Chim. Acta* **1969**, *3*, 89. (f) Abdur-Rashid, K.; Clapham, S. E.; Hadzovic, A.; Harvey, J. N.; Lough, A. J.; Morris, R. H. *J. Am. Chem. Soc.* **2002**, *124*, 15104. (g) Wigfield, D. C. *Tetrahedron* **1979**, *35*, 449.

(3) Related systems that partake in ligand-assisted ionic hydrogenations typically rely upon the ligand to deliver a protic hydrogen, while the metal hydride transfers to the electrophilic carbonyl position (i.e., the metal-hydride also acts as a nucleophile as in route **A**). See (a) Bullock, R. M. *Chem. - Eur. J.* **2004**, *10* (10), 2366. (b) Clapham, S. E.; Hadzovic, A.; Morris, R. H. *Coord. Chem. Rev.* **2004**, *248* (21−24), 2201. (c) Wang, D.; Astruc, D. *Chem. Rev.* **2015**, *115* (13), 6621.

(4) (a) Simpson, M. C.; Cole-Hamilton, D. J. *Coord. Chem. Rev.* **1996**, *155*, 163. (b) MacDougall, J. K.; Simpson, M. C.; Green, M. J.; Cole-Hamilton, D. J. J. *J. Chem. Soc., Dalton Trans.* **1996**, 1161. (c) Sola, M.; Ziegler, T. *Organometallics* **1996**, *15*, 2611. (d) Cheliatsidou, P.; White, D. F. S.; Slawin, A. M. Z.; Cole-Hamilton, D. J. *Dalton Trans.* **2008**, 2389. (e) MacDougall, J. K.; Simpson, M. C.; Green, M. J.; Cole-Hamilton, D. J. J. *J. Chem. Soc., Dalton Trans.* **1996**, 1161. (f) Fahey, D. R. *J. Am. Chem. Soc.* **1981**, *103*, 136. (g) Milstein, D. *J. Am. Chem. Soc.* **1986**, *108*, 3525.

(5) For examples, see (a) Peterson, E.; Khalimon, A. Y.; Simionescu, R.; Kuzmina, L. G.; Howard, J. A. K.; Nikonov, G. I. *J. Am. Chem. Soc.* **2009**, *131*, 908. (b) Sieffert, N.; Bühl, M. *J. Am. Chem. Soc.* **2010**, *132*, 8056. (c) Bosson, J.; Poater, A.; Cavallo, L.; Nolan, S. P. *J. Am. Chem. Soc.* **2010**, *132*, 13146. (d) Khalimon, A. Y.; Ignatov, S. K.; Simionescu, R.; Kuzmina, L. G.; Howard, J. A. K.; Nikonov, G. I. *Inorg. Chem.* **2012**, *51*, 754. (e) Wang, W.; Gu, P.; Wang, Y.; Wei, H. *Organometallics* **2014**, *33*, 847. (f) Iron, M. A.; Sundermann, A.; Martin, J. M. L. *J. Am. Chem. Soc.* **2003**, *125*, 11430.

(6) (a) Pruett, R. L. *Ann. N. Y. Acad. Sci.* **1977**, *295*, 239. (b) Feder, H. M.; Rathke, J. W. *Ann. N. Y. Acad. Sci.* **1980**, *333*, 45. (c) Fahey, D. R. *J. Am. Chem. Soc.* **1981**, *103*, 136. (d) Bradley, J. S. *J. Am. Chem. Soc.* **1979**, *101*, 7419. (e) Dombek, B. D. *J. Am. Chem. Soc.* **1980**, *102*, 6855. (f) Keim, W.; Berger, M.; Schlupp, J. *J. Catal.* **1980**, *61*, 359. (g) Daroda, R. J.; Blackborow, J. R.; Wilkinson, G. *J. Chem. Soc., Chem. Commun.* **1980**, 1098. (h) Daroda, R. J.; Blackborow, J. R.; Wilkinson, G. *J. Chem. Soc., Chem. Commun.* **1980**, *0*, 1101. (i) Paxson, T. E.; Reilly, C. A.; Holecek, D. R. *J. Chem. Soc., Chem. Commun.* **1981**, 618. (j) Knifton, J. F. *J. Chem. Soc., Chem. Commun.* **1981**, 188. (k) Backvall, J. E.; Akermark, B.; Ljunggren, S. O. *J. Am. Chem. Soc.* **1979**, *101*, 2411. (l) Roth, J. A.; Orchin, M. *J. Organomet. Chem.* **1979**, *172*, C27. (m) Sisak, A.; Sámpár-Szerencsés, E.; Galamb, V.; Németh, L.; Ungváry, F.; Pályi, G. *Organometallics* **1989**, *8*, 1096.

(7) (a) Vaughn, G. D.; Gladysz, J. A. *J. Am. Chem. Soc.* **1981**, *103* (18), 5608. (b) Garralda, M. A.; Hernández, R.; Ibarlucea, L.; Pinilla, E.; Torres, M. R.; Zarandona, M. *Organometallics* **2007**, *26*, 1031. (c) Van Voorhees, S. L.; Wayland, B. B. *Organometallics* **1985**, *4*, 1887. (d) Fu, X.; Basickes, L.; Wayland, B. B. *Chem. Commun.* **2003**, 520. (e) Fu, X.; Wayland, B. B. *J. Am. Chem. Soc.* **2005**, *127*, 16460.

DOI: 10.1021/acs.organomet.7b00158
Organometallics 2017, 36, 1609−1617

(f) Vaughn, G. D.; Strouse, C. E.; Gladysz, J. A. *J. Am. Chem. Soc.* **1986**, *108*, 1462. (g) Vaughn, G. D.; Gladysz, J. A. *J. Am. Chem. Soc.* **1986**, *108*, 1473. (h) Brockaart, G.; El Mail, R.; Garralda, M. A.; Hernández, R.; Ibarlucea, L.; Santos, J. I. *Inorg. Chim. Acta* **2002**, *338*, 249. (i) El Mail, R.; Garralda, M. A.; Hernández, R.; Ibarlucea, L.; Pinilla, E.; Torres, M. R. *Organometallics* **2000**, *19*, 5310.

(8) For current state-of-the-art, see (a) Nguyen, K. D.; Herkommer, D.; Krische, M. J. *J. Am. Chem. Soc.* **2016**, *138*, 14210. (b) Geary, L. M.; Glasspoole, B. W.; Kim, M. M.; Krische, M. J. *J. Am. Chem. Soc.* **2013**, *135*, 3796. (c) Patman, R. L.; Chaulagain, M. R.; Williams, V. M.; Krische, M. J. *J. Am. Chem. Soc.* **2009**, *131*, 2066.

(9) Jing, Q.; Sandoval, C. A.; Wang, Z.; Ding, K. *Eur. J. Org. Chem.* **2006**, *2006*, 3606.

(10) Nakamura, Y.; Yoshikai, N.; Ilies, L.; Nakamura, E. *Org. Lett.* **2012**, *14*, 3316.

(11) Saes, B. W. H.; Verhoeven, D. G. A.; Lutz, M.; Klein Gebbink, R. J. M.; Moret, M.-E. *Organometallics* **2015**, *34*, 2710.

(12) (a) Doyle, L. E.; Piers, W. E.; Borau-Garcia, J. *J. Am. Chem. Soc.* **2015**, *137*, 2187. (b) Doyle, L. E.; Piers, W. E.; Borau-Garcia, J.; Sgro, M. J.; Spasyuk, D. M. *Chem. Sci.* **2016**, *7*, 921.

(13) For examples, see (a) Bruce, M. I.; Hambley, T. W.; Snow, M. R.; Swincer, A. G. *J. Organomet. Chem.* **1982**, *235*, 105. (b) Akkerman, F. A.; Lentz, D. *Angew. Chem., Int. Ed.* **2007**, *46*, 4902. (c) Choi, J.-C.; Sarai, S.; Koizumi, T.; Osakada, K.; Yamamoto, T. *Organometallics* **1998**, *17* (10), 2037. (d) Nishihara, Y.; Yoda, C.; Itazaki, M.; Osakada, K. *Bull. Chem. Soc. Jpn.* **2005**, *78*, 1469. (d1) Bianchini, C.; Meli, A.; Peruzzini, M.; Vizza, F.; Frediani, P.; Ramirez, J. A. *Organometallics* **1990**, *9*, 226. (e) Tejel, C.; Geer, A. M.; Jiménez, S.; López, J. A.; Ciriano, M. A. *Organometallics* **2012**, *31*, 2895. (f) Carr, S. W.; Shaw, B. L.; Thornton-Pett, M. *J. Chem. Soc., Dalton Trans.* **1987**, 1763.

(14) (a) van der Boom, M. E.; Zubkov, T.; Shukla, A. D.; Rybtchinski, B.; Shimon, L. J. W.; Rozenberg, H.; Ben-David, Y.; Milstein, D. *Angew. Chem., Int. Ed.* **2004**, *43*, 5961. (b) Daugulis, O.; Brookhart, M. *Organometallics* **2004**, *23*, 527. (c) Pawley, R. J.; Huertos, M. A.; Lloyd-Jones, G. C.; Weller, A. S.; Willis, M. C. *Organometallics* **2012**, *31*, 5650.

(15) (a) Moxham, G. L.; Randell-Sly, H.; Brayshaw, S. K.; Weller, A. S.; Willis, M. C. *Chem. - Eur. J.* **2008**, *14*, 8383. (b) Arras, J.; Speth, H.; Mayer, H. A.; Wesemann, L. *Organometallics* **2015**, *34*, 3629. (c) Barthes, C.; Lepetit, C.; Canac, Y.; Duhayon, C.; Zargarian, D.; Chauvin, R. *Inorg. Chem.* **2013**, *52*, 48. (d) Lepetit, C.; Poater, J.; Alikhani, M. E.; Silvi, B.; Canac, Y.; Contreras-García, J.; Solà, M.; Chauvin, R. *Inorg. Chem.* **2015**, *54*, 2960. (e) Lesueur, W.; Solari, E.; Floriani, C.; Chiesi-Villa, A.; Rizzoli, C. *Inorg. Chem.* **1997**, *36*, 3354. (f) Logan, J. R.; Piers, W. E.; Borau-Garcia, J.; Spasyuk, D. M. *Organometallics* **2016**, *35*, 1279.

(16) Scherer, W.; Dunbar, A. C.; Barquera-Lozada, J. E.; Schmitz, D.; Eickerling, G.; Kratzert, D.; Stalke, D.; Lanza, A.; Macchi, P.; Casati, N. P. M.; Ebad-Allah, J.; Kuntscher, C. *Angew. Chem., Int. Ed.* **2015**, *54*, 2505.

(17) Kozuch, S.; Shaik, S. *Acc. Chem. Res.* **2011**, *44*, 101.

(18) Zhang, Y.; Lewis, J. C.; Bergman, R. G.; Ellman, J. A.; Oldfield, E. *Organometallics* **2006**, *25*, 3515.

(19) Goodman, J.; Grushin, V. V.; Larichev, R. B.; Macgregor, S. A.; Marshall, W. J.; Roe, D. C. *J. Am. Chem. Soc.* **2010**, *132*, 12013.

(20) (a) Minenkov, Y.; Occhipinti, G.; Jensen, V. R. *J. Phys. Chem. A* **2009**, *113*, 11833. (b) Zhao, Y.; Truhlar, D. G. *Org. Lett.* **2007**, *9*, 1967. (c) Sieffert, N.; Bühl, M. *Inorg. Chem.* **2009**, *48*, 4622. (d) McMullin, C. L.; Jover, J.; Harvey, J. N.; Fey, N. *Dalton Trans.* **2010**, *39*, 10833. (e) Ahlquist, M. S. G.; Norrby, P.-O. *Angew. Chem., Int. Ed.* **2011**, *50*, 11794.

(21) (a) Ahmad, N.; Levison, J. J.; Robinson, S. D.; Uttley, M. F.; Wonchoba, E. R.; Parshall, G. W. *Inorg. Synth.* **1990**, *28*, 81−83. (b) Jing, Q.; Sandoval, C. A.; Wang, Z.; Ding, K. *Eur. J. Org. Chem.* **2006**, *2006*, 3606−3616. (c) Nakamura, Y.; Yoshikai, N.; Ilies, L.; Nakamura, E. *Org. Lett.* **2012**, *14*, 3316−3319.

DOI: 10.1021/acs.organomet.7b00158
Organometallics 2017, 36, 1609−1617